Structural Analysis of Glulam Frame of a Modular Timber–Aluminium Hybrid Façade System in Nordic Climate

Katarzyna Ostapska, Johannes Brozovsky, Domas Valiukas, and Eimantas Tinginys

Contents

1 Introduction 1347
2 Methodology 1349
3 Results 1354
4 Discussion 1357
5 Conclusions 1357
References 1358

1 Introduction

The ongoing effort to limit emissions in the construction industry is now focusing on the embodied energy in building materials to introduce renewable and bio-based alternatives, such as engineered wood products (EWP), to building products traditionally made with concrete, steel, or aluminium. One such substitution is a façade system bearing frame structure commonly made in aluminium. While increasing the sustainability of source material performance requirements must still be met, and the minimum 35 years of service life should be ensured to qualify as carbon removal according to the new European certification scheme [1]. While certain system elements, that is insulated panels and glass panels attached to the timber frame, can be exchanged after 20–25 years [2], the structure should withstand at least two

K. Ostapska (✉) · J. Brozovsky
SINTEF Community, Trondheim, Norway
e-mail: katarzyna.ostapska@sintef.no

D. Valiukas · E. Tinginys
Staticus UAB, Vilnius, Lithuania

M. Kioumarsi, B. Shafei (eds.), *The 1st International Conference on Net-Zero Built Environment*, Lecture Notes in Civil Engineering 237,
https://doi.org/10.1007/978-3-031-69626-8_113

service lives and approach the typical building design service life of 100 years. The infill/insulation, sealing, and cladding elements that are subject to ever-increasing energy-efficiency and air and moisture tightness requirements should be installed allowing easy disassembly as specified in the standard ISO 20887:2020 [3]. Overall sustainability of the hybrid timber–aluminium façade system was shown to be superior to the aluminium-based system [2] via Life-Cycle Assessment including end-of-life scenarios of landfilling, recycling, and reuse. The benefits of the most preferable scenario, that is reuse, are subject to the uncertainties connected to the delayed realization and technical and economic feasibilities. To ensure the durability of the structural glulam façade frame with an accepted reliability level, real environmental loads should be considered and possibly adapted to include climate change scenarios. Wood exposed to moisture fluctuations over time can develop fungi, and rot and lose its functional properties. Timber can be effectively protected over many decades by providing proper façade insulation and ventilation based on good practice, as well as introducing predictive inner climate control via sensors. Especially challenging weather conditions can be experienced in Scandinavia, where high humidity and short dry seasons require climate-conscious adaptations of building solutions. Furthermore, coastal locations are exposed to high wind loads that lead to unavoidable fatigue-induced damages over longer periods. Fatigue in wood is a complex research field, where material anisotropy and typical huge variations of static mechanical properties hinder the development of universally applicable rules while accurate quantification of environmental and operational loads poses further challenges. Fatigue life is usually understood as the number of load cycles N at a given load amplitude S leading to the mechanical failure, where damage accumulates with every cycle and reaches value 1 at ultimate failure. Different fatigue lives for common wood failure modes found in literature and standards are shown in Fig. 1.

Load cycles differ in amplitude, frequency, form, direction, and distribution on the structure. Dynamically applied load, that is wind on facades is difficult to

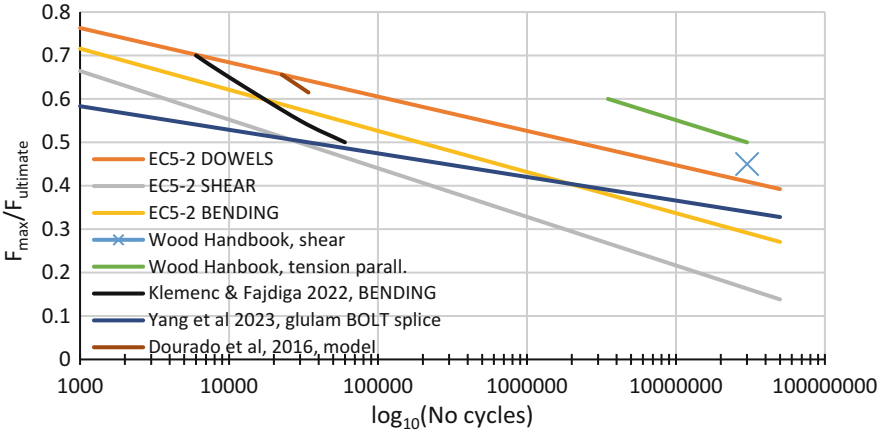

Fig. 1 Fatigue life curves for timber in literature [4–6] and EC5-2

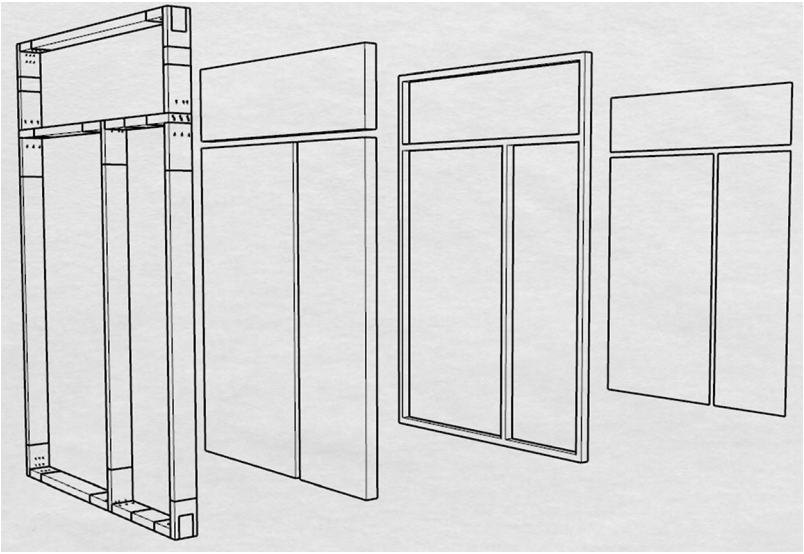

Fig. 2 Elements of the façade system from the left: timber frame, insulation, aluminium frame, and glass pack/metal panels

quantify due to varying directions and particular aerodynamic conditions in the area. Increased exposure to high wind loads can lead to decreased service life and premature damage. Damage in wood due to various cyclic loads is underdeveloped research area. Non-linear damage accumulation models require multitude long-duration cycling experiments for a given wood species. However, linear damage accumulation model of Palmgren-Miner was found to exhibit sufficient accuracy for timber roof-to-wall connections subjected to wind load [7]. This article presents the methodology of evaluating fatigue life of façade timber frame under wind loads and its practical application for three locations in Norway (Oslo, Trondheim, Tromsø) based on 3 years of wind observations (2021, 2022, 2023). The frame and façade system build-up is depicted in Fig. 2.

2 Methodology

To ensure the successful reuse of façade elements, the capacity to withstand several environmental loads must be sufficient. Most critical loads include cycling moisture and temperature changes and wind loads. The considered hybrid timber–aluminium façade system was already assessed as safe against mould development in Nordic climates [8, 9]. This study is devoted to the mechanical performance only and assumes sufficient biological decay resistance of timber frame over the 100-year period and proper maintenance and regular inspection or monitoring.

2.1 Experimental Tests of Timber Frame Connections

Experimental static mechanical tests were performed on the internal screw connections of the frame depicted in Fig. 3. The connections are loaded vertically, in the plane of the glulam frame and represent gravity loads. Three- and four-point bending tests were performed for L-joint and T-joint, respectively. Strain gauges were used to apply the load at the speed of 0.1 kN/s. Force and displacement data were logged.

L-joint consists of a 150 × 150 × 10 mm L-bracket and nine 45-degree inclined screws of 5 mm diameter and 50 mm length. T-joint features three rows of four 5 × 140 mm screws connecting three timber members at 45-degree to the wood fibre direction.

2.2 Numerical FEM of Experimental Tests of Joints

The finite element method was used to simulate the mechanical behaviours of the connection under the conditions of the laboratory test. Continuum 3D elements with eight nodes reduced integration and a general size of 5 mm were used. Mesh sensitivity was investigated to provide sufficient accuracy within reasonable

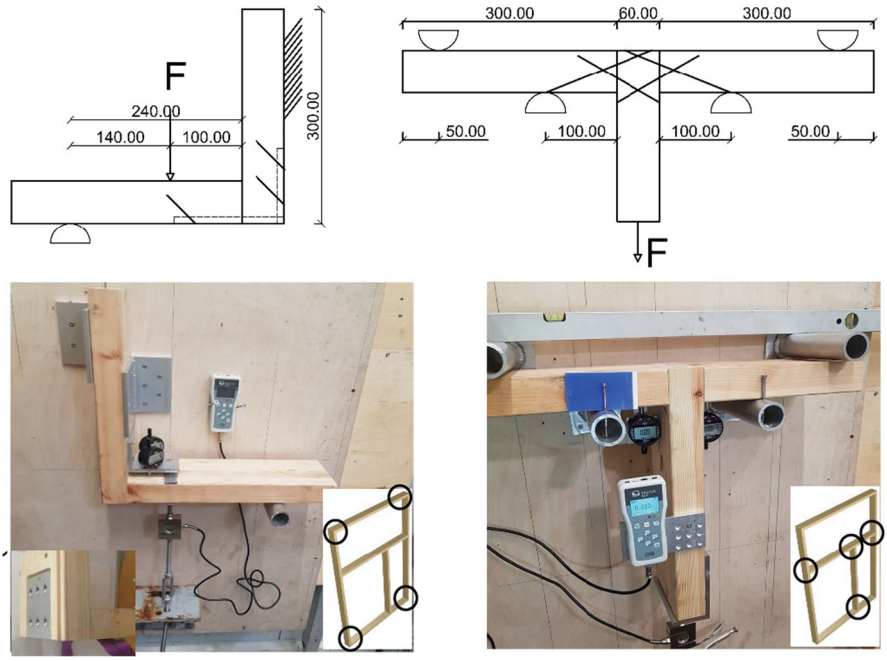

Fig. 3 Experimental setup scheme and photo for L-joint (left) and T-joint (right)

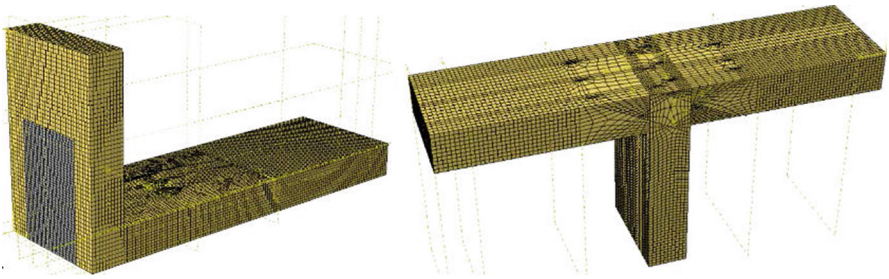

Fig. 4 Discretized numerical models of L-joint (left) and T-joint (right)

Table 1 Wood material model: elastic orthotropy constants for E modulus, Poisson ratio ν and shear modulus G, where L-longitudinal, R-radial, and T-tangential direction, f-strength

Stiffness	E_L	E_R	E_T	ν_{LR}	ν_{LR}	ν_{LR}	G_{LR}	G_{LT}	G_{RT}
[GPa]	10	0.79	0.34	0.5	0.66	0.84	0.64	0.58	0.03
Strength	$f_{L,t}$	$f_{L,c}$	$f_{R,t}$	$f_{R,c}$	$f_{T,tn}$	$f_{T,c}$	f_{LR}	f_{LT}	f_{RT}
[MPa]	63	−29	4.9	−3.6	2.8	−3.8	6.1	4.4	1.6

computation time. The discretization of the models is shown in Fig. 4. The wood material model is elastic orthotropy with nine parameters listed in Table 1.

Steel was modelled as elastic isotropic with $E = 210$ GPa, and $\nu = 0.3$. Screws are modelled without thread as a smooth shank of the screw core diameter and tied to wood.

2.3 Wind Load Model

Wind load calculations were carried out according to EN-1991-1-4 2005. The rules apply for buildings up to 200 m high. Basic wind velocity is obtained from the meteorological station (Oslo, Blindern) using API Frost as max wind velocity values in 10-min intervals at 10 m height above the ground and hourly mean velocity for reference, see Fig. 5.

Wind action on the façade is represented by the equivalent surface pressure q_p:

$$q_p(z) = \left[1 + \frac{k_r \cdot v_b \cdot k_l}{v_m(z)}\right] \cdot 0.5 \cdot \rho \cdot {v_m}^2(z), v_m(z) = k_r \cdot \ln\left(\frac{z}{z_0}\right) \cdot c_0(z) \cdot v_b \quad (1)$$

where in the function of height z in the coastal area with terrain category 0, where v_b is the base wind speed, see EN 1995-1 for details.

$$v_b = c_{\text{dir}} \cdot c_{\text{season}} \cdot v_{b,0} \quad (2)$$

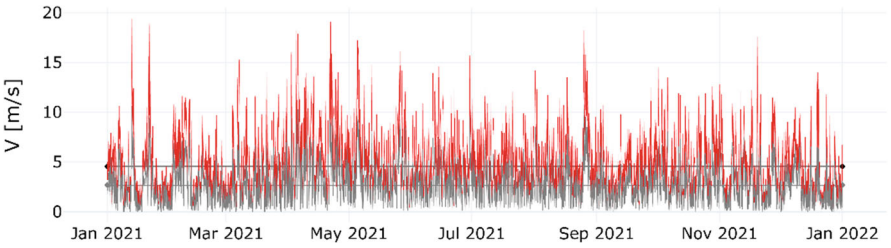

Fig. 5 Wind speed at 10-min temporal resolution (red—maximum peak, grey—mean) observed at Oslo-Blindern in 2021

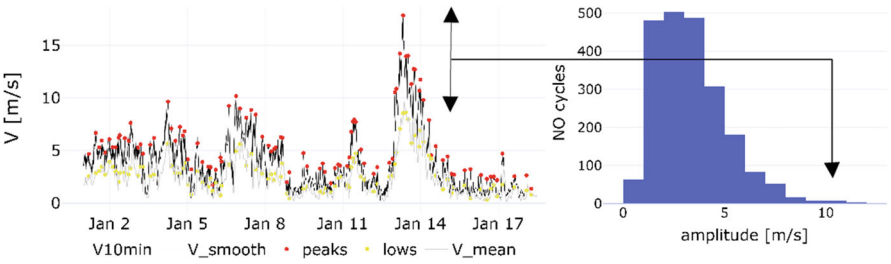

Fig. 6 Wind speed peaks (Oslo) identified from 10 min maximum values shown for 1 week (top) and amplitude histogram for all peaks during one year of data

where c_{dir}, c_{season}, are directional and seasonal wind factors, respectively. Wind load has a non-constant amplitude and requires handling damage accumulation from different cycles. Cycles are extracted from maximum wind time series using smoothing function (Savitzky-Golay filter within scipy package for Python 3) and peak (extremum) finding algorithm with peak prominence of minimum 1 m/s. The wind observations are available only for maximum and mean values at the highest 10-min resolution so the reference for amplitude estimation is chosen as the mean wind speed for each peak. Peaks and amplitude histograms for 10 amplitude ranges are depicted in Fig. 6.

2.4 Numerical Simulation of the Frame Under Static Equivalent Force

The model of the glulam frame for structural analysis with FEM was created within commercial software ABAQUS, see Fig. 7. The connection models validated with experimental tests for T-joint and L-joint were embedded in the frame model. The frame was fixed by T-plates on the top and horizontal translations are blocked at the bottom beam where bolted locks are attached. Pressure is collected from the frame

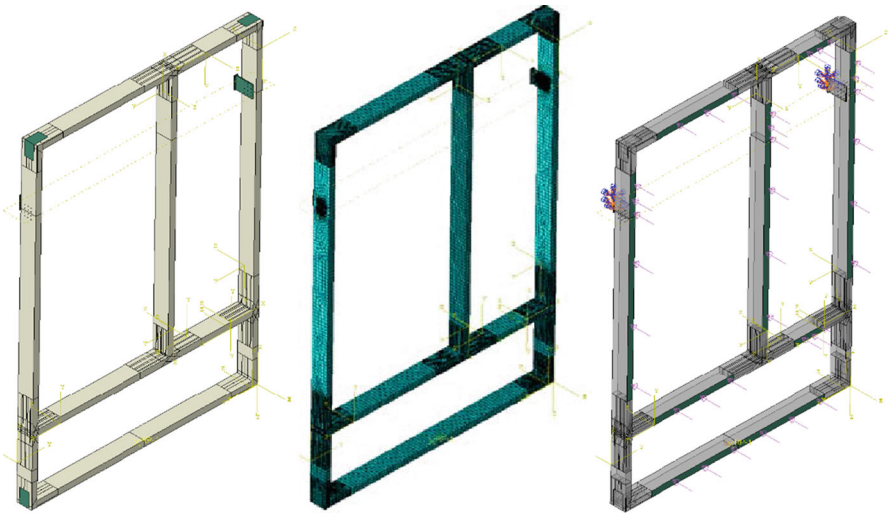

Fig. 7 Geometry, mesh, and boundary conditions of the glulam frame model for FEA

façade surface 2.45 × 3.4 m^2 and distributed over the front frame surface. The weight of the façade panels is not applied, and only the self-weight of timber and steel is considered.

Fatigue verification for timber structures is usually based on a simplified method from EN 1995-2-2, Annex A assuming equivalent constant amplitude fatigue loading. When several different loading amplitudes are present cumulative damage can be evaluated according to Palmgren-Miner theory of linear cumulative damage, see Eq. 3, where D denotes damage, N_{tot} is the total number of cycles, n_i is the stress level of a given load cycle i, and $N_{f,i}$ is the fatigue life corresponding to stress level n_i.

$$D = \sum_{i=1}^{N_{\text{tot}}} \frac{n_i}{N_{f,i}}, D \in <0, 1> \tag{3}$$

Information about damage induced by each load cycle is required and is evaluated by inverting EC5 formula to obtain fatigue life for a k stress level:

$$D \log(N_i) = (1 - k_i) \frac{a(b - R)}{1 - R}, R = \frac{\sigma_{d,\min}}{\sigma_{d,\max}} \tag{4}$$

Stress levels k_i is directly extracted from the wind history as wind peaks ratio to the maximum allowed wind capacity. Coefficients a and b representing the type of fatigue are chosen for dowel-type connections according to Table A.1 in EC5-2 (EN 1995-2-2). R is defined as a ratio of minimum to maximum design stress applied in the load cycle. Fatigue material factor is not accounted for.

3 Results

3.1 *Experimental and Numerical Results for Timber Frame Connections*

Force–displacement curves from connections experiment and simulation show good agreement in the elastic range, see Fig. 8. L-connection experiences slip, not captured by the simulation but measured at around 0.26 mm. The slip is caused by the presence of the L-shaped, 15 × 15 × 1 cm steel plate connecting frame corner elements.

3.2 *Numerical Simulation of Timber Frame and Fatigue Service Life Estimation*

The final maximum basic wind speed for building height 12 m (third story) was 19.4 m/s and corresponds to the pressure of around 6.8 kPa. Under this statically applied pressure, the frame timber members reach 28% capacity in compression perpendicular to the grain around the T-plate bolts, see Fig. 9.

The central T-joint is the most strained connection in the frame and perpendicular to grain compression stresses are at 3 MPa and 83% capacity. L-joint has the largest value of longitudinal shear stresses with 30% capacity (see Table 2), while compression perpendicular to the grain is at 22%, see Fig. 9. Stresses in steel elements under maximum load are depicted in Fig. 10. Mises stress hypothesis was used to estimate stress level in T-brackets, L-joint, and T-joint. Most stressed steel elements are bottom bolts and the bottom part of the T-bracket that transfer most of the load of the timber frame hanging on them. However, the level of stress at just below 160 MPa was found to be below 50% of the ultimate tensile strength limit for the most typical carbon steel of grade S235, namely 360 MPa. Such a low level of stress allows us to assume that load in steel elements is below the endurance limit for fatigue defined in Eurocode 3, part 1–9 (EN 1993-1-9).

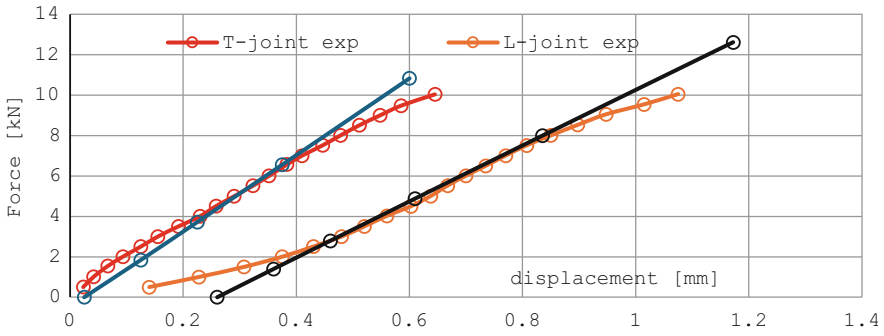

Fig. 8 Load–displacement curves for T-joint and L-joint in glulam frame from experiment (red, orange) and numerical simulation (blue, black)

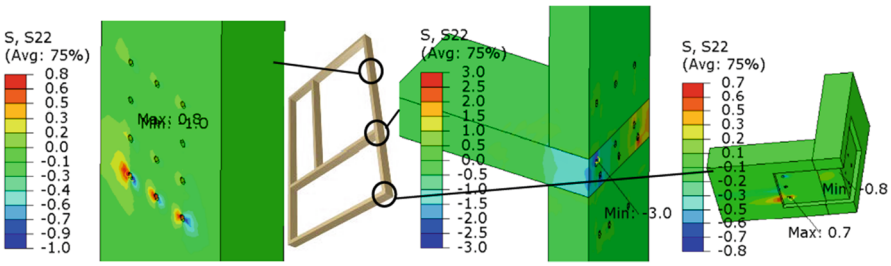

Fig. 9 Stress in timber perpendicular to grain around T-plate bolts at ca 28% capacity (left), 83% in T-joint (middle), and 22% in L-joint (right)

Table 2 Max stresses from FEA for each material direction and corresponding usage

Element		$\sigma_{L,t}$	$\sigma_{L,c}$	$\sigma_{R,t}$	$\sigma_{R,c}$	$\sigma_{T,t}$	$\sigma_{T,c}$	σ_{LR}	σ_{LT}	σ_{RT}
Beams	[MPa]	3.7	−4.9	0.8	−1	0.1	−0.2	1.3	0.4	0.1
	[−]	6%	17%	16%	28%	4%	5%	21%	9%	6%
T-joint	[MPa]	3.4	−3.4	3	−3	0.5	−0.5	1.7	0.6	0.4
	[−]	5%	12%	61%	83%	18%	13%	28%	14%	25%
L-joint	[MPa]	4.8	−4.5	0.7	−0.8	0.8	−0.9	0.7	1.3	0.4
	[−]	8%	16%	14%	22%	29%	24%	11%	30%	25%

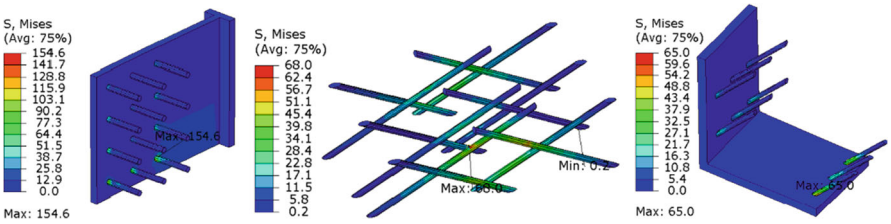

Fig. 10 Mises stress in steel T-plate bolts at ca 80% yield limit capacity (left), 36% in T-joint (middle), and 34% in L-bracket screws (right)

Maximum deformations of 4.8 mm occur in T-joint as shown in Fig. 11.

The wind speed at which the frame is at 100% of local static perpendicular to grain compressive stress capacity is set at 19.4/0.83 = 23.5 m/s. Additionally, to account for the higher dynamic elastic modulus, the maximum wind speed was increased by 20% to 28.2 m/s. The value was based on the literature findings, where a different mean ratio between dynamic and static modulus of elasticity for wood was found, that is 1.07 [10], 1.1 [11], 1.13 [12], 1.22 [13], and 1.28 [14]. All identified load cycles are considered for total damage evaluation without assuming fatigue endurance limit. Cumulative linear damage for four consecutive years 2020–2023 in three Nordic cities is summarized in Table 3. Based on those damages, the predicted service life due to mechanical fatigue failure in the frame is estimated for each location at over 100 years for both Oslo and Trondheim and at 32 years for Tromsø.

Overview of load cycles due to wind for a given year is shown in Fig. 12.

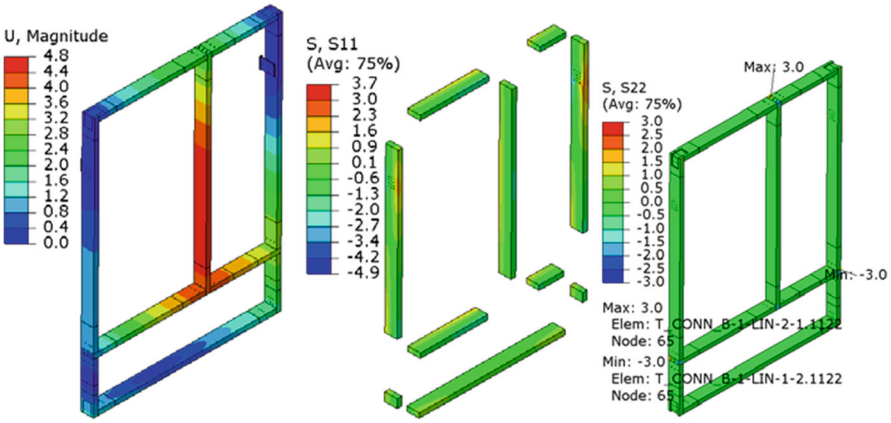

Fig. 11 Deformations [mm] of the frame under 6.8 kPa pressure (left), bending stresses in beams (middle), max perpendicular to grain stresses in joints (right) [MPa]

Table 3 Cumulative linear damage due to wind-induced fatigue

		Damage		
	Year	Oslo	Trondheim	Tromsø
	2020	7.58E–06	7.63E–05	1.05E–01
	2021	1.91E–06	4.45E–04	5.88E–03
	2022	4.33E–05	4.45E–04	1.28E–02
	2023	3.28E–07	3.63E–05	2.19E–03
Total damage		5.31E–05	1.00E–03	1.26E–01
Predicted service life		>100	>100	32

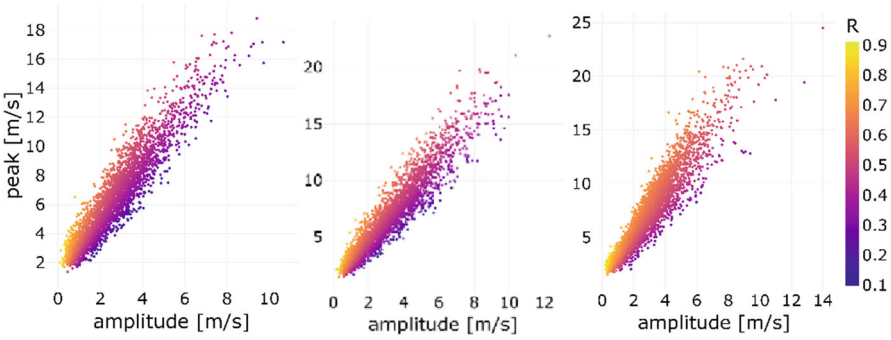

Fig. 12 Total yearly (2021) wind load cycles by amplitude and peak speed, color-coded by R value for Oslo (left), Trondheim (middle), and Tromsø (right)

4 Discussion

4.1 Discussion of Results

Service life due to damage accumulation in timber frame under wind exposure is estimated as non-critical for Oslo (Blindern) and Trondheim (Voll) observations assuming a height of 12 m above the ground. Tromsø location has a decidedly smaller service life, at 32 years. The main factor is the presence of several high peaks in wind speed compared to the estimated frame capacity of 28.5 m/s. For the more exposed locations with direct seaside locations, and stronger winds design changes are recommended, for example symmetric geometry or stiffening elements. Furthermore, experiments on the out-of-plane load response of both T-joint and L-joint would improve the estimation of capacity and service life.

4.2 Limitations of the Research

This work makes several limiting assumptions. Only static structural analysis is performed, and no dynamic effects and time-dependent material properties are accounted for in the simulation. Moisture-induced stresses, damage due to moisture cycles, and coupled moisture-mechanical stress fields were not considered. Wind loads are collected from 10 min frequency data of maximum wind speeds. Thus, actual number of cycling and real minimum wind speed for accurate amplitude estimation is not known. Wind direction was not accounted for to decrease the real pressure on the façade, which is a conservative assumption. The positive stiffening effect of façade panels was not included, and fatigue of steel T-plate connectors and screws was not studied in detail due to the assumed endurance limit at the expected stress level. Additionally, the cumulative damage was obtained based on linear theory, and the progressive increase in the damaging effect of similar cycles was not considered. The influence of the accumulated damage and duration of load can be substantial factors for fatigue life assessment. However, no sufficient data for the wood performance under different sequences of short-term loading are available in the standards and literature to allow for a non-linear damage accumulation model with a sufficient confidence level. Thus, the focus of future research within timber engineering should be damage development and accumulation under cycling loading if carbon removal goals in timber construction are to be achieved.

5 Conclusions

Structural analysis of the glulam frame supporting a novel modular façade system in the Nordic wind conditions was performed to predict fatigue service life to ensure the long-term sustainability of replacing aluminium/steel with glulam. The finite

element model of the frame was calibrated using laboratory mechanical tests of the T- and L-joint with screws and brackets. Continuum models of both timber and steel were used to increase the precision of modelling complex stress states for the identification of failure modes. Linear damage accumulation calculation is shown for 4 years between 2020 and 2023 in Oslo, Trondheim, and Tromsø locations in Norway. Key conclusions from the paper are listed:

- The critical role of the major wind load events with speed over 20 m/s on the fatigue life and damage in timber frame is observed.
- Design alternation, that is introducing symmetrical geometry, re-designing, or reinforcing joint is recommended to limit the load level in the critical location.
- The most critical failure mode was identified as local perpendicular to grain compression in wood in the T-joint.
- The predicted service fatigue life for the façade system is estimated at 32 years for Tromsø and over 100 years for Oslo and Trondheim.

Acknowledgements This research was funded by the EEA Norway Grant nr LT-INNOVATION-0002: 'Developing a more environmentally friendly automated façade system that is integrated into the building's control systems'. Experimental tests were performed in 2022.

References

1. Commission welcomes political agreement on EU-wide certification scheme for carbon removals. https://ec.europa.eu/commission/presscorner/detail/en/ip_24_885, released 2024/02/20
2. Cheong, C.Y., Brambilla, A., Gasparri, E., Kuru, A., Sangiorgio, A.: Life cycle assessment of curtain wall facades: a screening study on end-of-life scenarios. J. Build. Eng. **84**, 108–600 (2024)
3. ISO 20887: Sustainability in buildings and civil engineering works—design for disassembly and adaptability—principles, requirements and guidance (2020)
4. Klemenc, J., Fajdiga, G.: Statistical modelling of the fatigue bending strength of Norway spruce wood. Materials. **15**, 536 (2022)
5. Yang, L., Chen, A., Zhou, J., He, G., Wang, H., Li, C.: Flexural fatigue behavior of glulam beams connected with steel splints and bolts. Buildings. **13**(5), 1218 (2023)
6. Dourado, N., de Moura, M.F.S.F., de Jesus, A.: Fatigue-fracture characterization of wood under mode I loading. Int. J. Fatigue. **121**, 265–271 (2019)
7. Alhawamdeh, B., Shao, X.: Fatigue performance of wood frame roof-to-wall connections with elastomeric adhesives under uplift cyclic loading. Eng. Struct. **229**, 111602 (2021)
8. Ostapska, K., et al.: Development of climatic damage predictive tool for timber façade moisture-related damage. J. Phys. Conf. Ser. **2600**(16), 162002 (2023)
9. Coelho, G.B.A., Kraniotis, D.: A multistep approach for the hygrothermal assessment of a hybrid timber and aluminium based facade system exposed to different sub-climates in Norway. Energ. Build. **296**, 113368 (2023)
10. Haines, D.W., Leban, J.M., Herbé, C.: Determination of Young's modulus for spruce, fir and isotropic materials by the resonance flexure method with comparisons to static flexure and other dynamic methods. Wood Sci. Technol. **30**, 253–263 (1996)

11. Spycher, M., Schwarze, F., Steiger, R.: Assessment of resonance wood quality by comparing its physical and histological properties. Wood Sci. Technol. **42**, 325–342 (2008)
12. Divos, F., Tanaka, T.: Relation between static and dynamic modulus of elasticity of wood. Acta Silv. Lign. Hung. **1**, 105–110 (2005)
13. Buron, I.: Modulus of elasticity of Norway spruce using different techniques. Master thesis, Lund University of Technology (1998)
14. Chauhan, S., Sethy, A.: Differences in dynamic modulus of elasticity determined by three vibration methods and their relationship with static modulus of elasticity. Maderas. Ciencia y Tecnología. **18**, 373 (2016)